11785 Final Project Report for Team 28

Frank Hu
Carnegie Mellon University
Pittsburgh, PA 15213
zhemingh@andrew.cmu.edu

Sungmyeon Park
Carnegie Mellon University
Pittsburgh, PA 15213
sungmyep@andrew.cmu.edu

Lehong Wang
Carnegie Mellon University
Pittsburgh, PA 15213
lehongw@andrew.cmu.edu

Zepeng Zhao
Carnegie Mellon University
Pittsburgh, PA 15213
zepengz@andrew.cmu.edu

Abstract

Automated defect detection in Printed Circuit Boards (PCBs) is essential for ensuring the quality and reliability of electronic components. This project leverages a dataset from Peking University's Open Lab on Human Robot Interaction, containing six types of PCB defects: missing holes, mouse bites, open circuits, shorts, spurs, and spurious copper. High-resolution images from this dataset were augmented and processed into 600×600 sub-images, resulting in a training set of over 10,000 samples.

We employ a Single Shot MultiBox Detector (SSD) with a ResNet50 backbone for defect classification and localization. The model achieved an overall accuracy of 93.02% and a test loss of 0.2216, demonstrating robust performance across defect types. Class-specific analysis revealed that the model performed best on missing holes and faced challenges with mouse bites. These results indicate strong generalization with minimal overfitting, as reflected in balanced training and validation metrics.

Future improvements will focus on enhancing the model's precision for challenging classes through advanced feature extraction and additional data augmentation. This work underscores the potential of deep learning in PCB defect detection, contributing to efficient quality control in electronics manufacturing.

1 Introduction

This project aims to enhance Printed Circuit Board (PCB) defect detection using advanced image-based techniques. Given that PCBs are the backbone of modern electronics, defects like open circuits and scratches can lead to significant performance issues. Current research emphasizes the need for more accurate and reliable inspection systems to reduce such defects.

Zhou et al. [27] discuss advancements in vision-based defect detection, particularly the use of automated optical inspection (AOI) systems and machine learning for image recognition, which are essential for improving defect detection accuracy. Wei et al. [22] demonstrated the superiority of convolutional neural networks (CNNs) over traditional methods, achieving high accuracy in classifying PCB defects.

However, these studies are conducted with an assumption of balanced and clean data with labeling. In most industry applications, obtaining manual labels for such datasets is often costly and time-consuming. As the result, performance of pre-mentioned models are induced by noise introduced by ambiguous labels, environmental conditions, and inevitably unbalanced data .[18] Researchers like

Preprint. Under review.

Silva et al.[17] have introduced methods that make model robust against noisy labels, and Strelcenia et al.[19] surveyed several methods that mitigate the effect of unbalanced data by generating imaginary data with Generative Adversarial Networks (GAN).

Inspired by these previous works, we aim to address similar problems of noised and unbalanced data for circuit defect detection tasks. The dataset used for this study consists of inspection and reference images, with various defect types such as PSR peel-off, pollution, foreign particles, and scratches labeled for analysis. By refining defect detection methods and improving the classification of smaller or less obvious defects, the project aims to contribute to more efficient manufacturing processes and higher product reliability in the electronics industry.

2 Literature Review

In this section, we will discuss three types of PCB defect detection solutions [3]: one-stage, two-stage, and transformer-based algorithms. One-stage algorithms, known for their high detection accuracy and speed, are particularly suited to real-time PCB defect detection. In contrast, two-stage algorithms, although typically slower, excel in detecting intricate defects due to their superior accuracy, making them popular in applications where speed is less critical. Transformer-based algorithms, using transformer models as the backbone, are also rapidly evolving. Additionally, transformer models have shown impressive performance in other fields, suggesting strong potential for PCB defect detection.

2.1 One-Stage Algorithms

Single-stage algorithms, notably represented by the single shot multibox detector (SSD) [10] and You Only Look Once (YOLO) [13] [14]. The YOLO algorithm offers a unique approach by framing target detection as a regression problem. It does this by dividing the input image into a grid and simultaneously predicting the class and bounding box attributes for multiple targets within each grid cell. YOLO performs target detection in a single-shot forward propagation pass, making it exceptionally fast, though it may be less effective for small target detection. Similarly, SSD predicts target classes and bounding boxes on feature maps at different scales, accommodating various target sizes through multiple anchor boxes of different dimensions. This design enables SSD to perform well with small and multi-scale targets.

To address stability and accuracy issues in PCB defect detection models, Xin et al. [24] introduced an improved YOLOv4 model. This model uses mosaic data augmentation during input processing and replaces the leaky rectified linear unit (Leaky-ReLU) activation in the network backbone with the Mish activation function. Similarly, to tackle the challenge of detecting small defects against complex PCB backgrounds, Zhang et al. [26] proposed a lightweight single-stage defect detection network. This network incorporates a dual attention mechanism and a path-aggregation feature pyramid network (PAFPN) to improve the detection of small defects. MobileNetV2, a lightweight backbone neural network, replaces ResNet101, significantly reducing model parameters, while the dual attention mechanism ensures efficient feature extraction. Li et al. [7] developed a dataset for PCB assembly scene object detection to address detection challenges related to anchor box sizes.

Wan et al. [20] proposed a defect detection method with a data-expanding strategy (DE-SSD) and evaluated it using YOLOv5 on both labeled and unlabeled samples. This approach reduces dependency on labeled data by utilizing both types of samples, while the data-expanding strategy helps mitigate the challenges posed by unlabeled data. The improvement is particularly noticeable with smaller data volumes, although the effect decreases as data size increases. In a related study, Wu et al. [23] introduced GSC YOLOv5, a deep learning detection method combining a lightweight network with a dual-attention mechanism. This modified algorithm integrates Ghost Conv and Ghost Bottleneck structures to significantly reduce model parameters and floating-point operations. The inclusion of SE and CBAM modules further enhances accuracy and detection speed. Zhao et al. [21] extended YOLOv5 by incorporating adaptive spatial feature fusion (ASFF) [9], allowing adaptive fusion of feature information across different spatial levels. Additionally, they introduced the global attention mechanism (GAM) to boost the model's information extraction capabilities. Lim and colleagues [8] developed a novel multi-scale feature pyramid network using YOLOv5, specifically targeting the detection of tiny PCB defects by leveraging contextual insights. This network also integrates the CIoU loss function to improve the precision of spatial parameter estimation, effectively pinpointing defect locations.

In summary, these studies have made notable advancements in PCB defect detection using one-stage algorithms. Innovations include attention mechanisms, data enhancement strategies, and advanced backbone networks. However, challenges remain, including reduced performance in complex defect scenarios, high dependence on limited sample data, and the need for further improvements to handle varied angles and lighting conditions effectively.

2.2 Two-Stage Algorithms

While single-stage algorithms offer faster processing, two-stage algorithms are known for their superior detection accuracy. Prominent two-stage algorithms include Region CNN (R-CNN) [5], Fast R-CNN [4], Faster R-CNN [15], and Mask R-CNN [6]. These approaches divide PCB defect detection into two phases: first, region proposal (RP), where pre-selected boxes are generated to identify areas likely containing defects; second, classification is performed on these regions using CNNs.

The R-CNN algorithm begins by creating a series of candidate regions (Region Proposals) within the input image. Each region undergoes CNN feature extraction, and the resulting features are passed to classifiers and bounding box regressors for target detection. While R-CNN achieves high accuracy, its speed is limited due to the need for separate CNN feature extraction for each candidate region. Faster R-CNN, an improved version, introduces the region proposal network (RPN), a learnable network designed to quickly generate candidate regions. By seamlessly integrating the RPN with classifiers and bounding box regressors, Faster R-CNN forms an end-to-end detection network, enabling candidate region generation and feature extraction within a single network and substantially improving detection speed.

In summary, while fewer studies focus on two-stage algorithms compared to one-stage approaches, two-stage methods clearly offer advantages in detection accuracy. Recently, one-stage algorithms have become popular due to their ability to meet real-time detection speed requirements, with only a slight difference in accuracy compared to two-stage algorithms. Consequently, there is relatively less research centered on two-stage methods.

2.3 Transformer-Based Algorithms

Although transformers have shown strong performance in computer vision (CV) and natural language processing (NLP), they face limitations in visual inspection tasks, particularly due to time constraints. These challenges have led to limited research on transformer applications in PCB defect detection. However, despite these barriers, recent studies have begun exploring ways to overcome these limitations, aiming to fully leverage transformer capabilities for PCB defect detection.

Despite the limited use of transformers in PCB defect detection, advancements in computer vision and computational power have driven the development of numerous transformer models. In 2021, Liu et al. [12] trained a Swin Transformer v2 model with three billion parameters, incorporating post-normalization and scaled cosine attention techniques. This model achieved state-of-the-art (SOTA) results across various visual tasks. As of 2023, the Swin Transformer v2 backbone network remains an active research area, consistently demonstrating exceptional performance.

An et al. [1] introduced a label-robust and patch-correlation-enhanced ViT (LPViT). Their ViT model, based on LPViT principles, emphasizes robustness and leverages relationships among distinct regions of PCB images. Additionally, random masking or substitution of certain blocks enhances the mutual understanding of different image regions. Chen [2] employed an enhanced clustering algorithm to generate optimized anchor frames tailored to the PCB defect dataset. In this approach, CNNs were replaced with a shifted window transformer (Swin Transformer) for network feature extraction, and channel ordering in the feature map was adjusted to allow the network to prioritize more valuable information. Yang et al. [25] proposed an enhanced YOLOv7 model with the SwinV2_TDD module, which includes an added convolutional layer to facilitate local PCB information extraction.

These innovative transformer models, designed for visual macro-models, capture multi-scale features and excel in dense prediction tasks. Such capabilities are intrinsic to transformer-based PCB defect detection, highlighting transformers' potential in this field.

2.4 Summary

In comparing two-stage and single-stage algorithms, the two-stage algorithm offers higher accuracy but is time-consuming, making it unsuitable for real-time detection tasks. In contrast, the single-stage algorithm is faster but has relatively lower accuracy. Transformer-based PCB target detection algorithms, built on the Transformer architecture, achieve excellent detection accuracy; however, they have slower detection speeds, require higher computational resources for training, and depend on large amounts of data.

3 Baseline Model

3.1 Baseline Selection

The 2023 study by Sharma et al. [16] establishes SSD ResNet50 as the baseline model and serves as the baseline paper for PCB defect detection, highlighting the effectiveness of ResNet50's deep residual network for this task. With its 50-layer architecture, ResNet50 excels in feature extraction by enabling the propagation of gradients through residual connections, which mitigates issues such as vanishing gradients. This structure is particularly valuable in PCB defect detection, where subtle variations in defect patterns, like minor scratches or PSR peel-off, require nuanced and detailed feature extraction to achieve high classification accuracy [6].

While the SSD framework adds efficiency by combining localization and classification in a single-stage approach, the ResNet50 backbone is the core of this model's strength. Its robust feature representation and deep layer structure allow it to capture high-level semantic features, making it well-suited for distinguishing complex defect types. This depth enables precise localization of defect regions, even in high-resolution images, supporting applications where timely and accurate defect identification is essential to maintaining manufacturing quality and throughput [11].

As the baseline model validated by Sharma et al. [16], SSD ResNet50 leverages ResNet50's powerful feature extraction capabilities, making it a reliable solution for real-time PCB quality control. Its adoption as a baseline in defect detection research underscores ResNet50's advanced capacity to handle high-dimensional, complex data—meeting the stringent demands of industrial-scale PCB inspection.

3.2 Baseline Model Description

ResNet50 is a 50-layer deep residual network known for its powerful feature extraction capabilities, making it well-suited for complex image classification tasks. With residual connections that facilitate efficient gradient flow, ResNet50 enables deep and nuanced feature representation, capturing intricate details essential for distinguishing subtle variations, such as those found in PCB defects. This depth and robustness in feature extraction allow ResNet50 to handle high-dimensional data with precision, making it an ideal choice for tasks requiring high accuracy and reliability. When paired with detection frameworks, such as SSD, ResNet50 becomes highly effective for real-time inspection applications.

3.3 Mathematical Description

Given an input printed circuit board (PCB) image $X \in \mathbb{R}^{H \times W \times C}$, we perform feature extraction using a ResNet-50 network. Let $f_{\text{ResNet}} : \mathbb{R}^{H \times W \times C} \to \mathbb{R}^{h \times w \times d}$ denote the feature extraction process, yielding the feature map $F \in \mathbb{R}^{h \times w \times d}$ such that:

$$F = f_{\text{ResNet}}(X)$$

where h and w are the spatial dimensions of the feature map, and d is the feature depth.

To detect objects within the PCB image, the base model apply the Single Shot MultiBox Detector (SSD)[11] approach on the feature map F. The SSD process involves the following steps:

1. Anchor Boxes: We define a set of anchor boxes, also known as *default boxes*, at each spatial location of F. Let $\mathcal{A} = \{(x_i, y_i, w_i, h_i)\}_{i=1}^{M}$ denote the set of anchor boxes, where (x_i, y_i) are the center coordinates, and w_i and h_i are the width and height of the i-th anchor box. Each anchor box has a predefined aspect ratio and scale.

2. Offset and Class Prediction: For each anchor box $(x_i, y_i, w_i, h_i) \in \mathcal{A}$, SSD predicts:

- Class probabilities $\mathbf{p}_i = (p_{i,1}, p_{i,2}, \ldots, p_{i,C+1}) \in \mathbb{R}^{C+1}$, representing the probability distribution over C object classes and an additional background class.
- Bounding box offsets $\mathbf{d}_i = (t_{x,i}, t_{y,i}, t_{w,i}, t_{h,i}) \in \mathbb{R}^4$, which are adjustments to the center coordinates and dimensions of the anchor box, refining it to fit detected objects.

3. Loss Function: The objective function for SSD is a weighted sum of the classification and localization losses, applied across all anchor boxes:

$$L = \frac{1}{N}\left(L_{\text{conf}} + \alpha L_{\text{loc}}\right)$$

where N is the number of matched anchor boxes, and α is a weighting factor. The components of the loss function are defined as follows:

- Classification Loss L_{conf}: This is a cross-entropy loss applied to the predicted class probabilities $\mathbf{p}_i$ for each anchor box, defined as:

  $$L_{\text{conf}} = -\sum_{i=1}^{M}\sum_{c=1}^{C+1} y_{i,c}\log(p_{i,c})$$

  where $y_{i,c}$ is the ground truth label (one-hot encoded) for class c of anchor box i.
- Localization Loss L_{loc}: This is a Smooth L1 loss applied to the bounding box offsets for the matched anchor boxes:

  $$L_{\text{loc}} = \sum_{i=1}^{M}\sum_{m\in\{x,y,w,h\}} \text{SmoothL1}(\hat{d}_{i,m} - d_{i,m})$$

  where $\hat{d}_{i,m}$ is the predicted offset and $d_{i,m}$ is the ground truth offset for anchor box i along dimension m, and the Smooth L1 loss is defined as:

  $$\text{SmoothL1}(x) = \begin{cases} 0.5x^2 & \text{if } |x| < 1 \\ |x| - 0.5 & \text{otherwise} \end{cases}$$

4. Final Detection: After computing the class probabilities and bounding box offsets, Non-Maximum Suppression (NMS) is applied to eliminate redundant detections, retaining only the highest-confidence predictions for each detected object. This completes the SSD-based object detection process for the PCB image.

4 Baseline Implementation

The proposed approach for printed circuit board (PCB) defect classification leverages a transfer learning strategy using the ResNet-50 architecture. The primary objective is to detect and classify six common defect types: mouse bites, shorts, open circuits, spurs, missing holes, and spurious copper. The implementation consists of data preprocessing, model training, evaluation, and visualization components.

4.1 Data Preparation and Preprocessing

The dataset was sourced from PCB images formatted following the PASCAL VOC structure. Image annotations were stored in XML format, containing detailed defect class information. The PCB Dataset class was created to load images and their respective labels by parsing the XML annotation files. The images were transformed using standard normalization and resizing operations to ensure compatibility with ResNet-50, which requires 224×224 pixel inputs.

Key transformations included:

- **Resize**: Images were resized to 300×300 pixels.
- **Normalization**: Mean and standard deviation values specific to ImageNet were applied for data normalization.

4.2 Model Architecture

The ResNet-50 model, pre-trained on ImageNet, was adapted for multi-class classification by modifying its final fully connected layer. The original output layer was replaced with a new linear layer to output predictions for six classes. This adaptation retained the feature extraction capabilities of ResNet-50 while fine-tuning the network for PCB defect classification.

4.3 Training Process

The model was trained using the following settings:

- **Optimizer**: AdamW optimizer with a learning rate of 0.0001.
- **Loss Function**: Cross-entropy loss.
- **Scheduler**: A ReduceLROnPlateau scheduler was employed to reduce the learning rate when the validation loss plateaued, ensuring stable convergence.
- **Batch Size**: 256 for training and testing, with 8 for validation.

Training and evaluation metrics were tracked for each epoch, including overall and per-class accuracy, and loss.

5 Baseline Model Evaluation

The classification model was trained and evaluated on a dataset consisting of six defect classes: Mouse Bites, Shorts, Open Circuits, Spurs, Missing Holes, and Spurious Coppers. The evaluation metrics include per-class accuracy and loss, overall accuracy, and loss trends during training and validation.

5.1 Per-Class Test Performance

The performance across the different classes was evaluated using accuracy and loss. The results show a variance in model effectiveness across the defect types:

- **Mouse Bites:** The model achieved an accuracy of 89.55% with a test loss of 0.2928. This indicates a relatively high loss compared to other classes, which suggests that Mouse Bites were among the more challenging classes for the model to classify accurately.
- **Shorts:** The accuracy was 91.93% with a loss of 0.2679. While the accuracy is above 90%, the associated loss highlights some classification uncertainty.
- **Open Circuits:** This class performed well with an accuracy of 93.64% and a test loss of 0.2229, showing that the model handled these defects effectively.
- **Spurs:** Achieved an accuracy of 90.68% and a test loss of 0.2706, comparable to the Shorts class.
- **Missing Holes:** This was the best-performing class with a high accuracy of 98.64% and the lowest test loss of 0.0334, indicating that the model had a strong ability to correctly identify these defects.
- **Spurious Coppers:** An accuracy of 94.01% and a loss of 0.2412, showing robust performance with moderate confidence.

5.2 Overall Model Performance

The overall test accuracy reached 93.02%, demonstrating that the model generalizes well across the dataset. The final overall test loss was 0.2216, reflecting the model's effective minimization of classification errors.

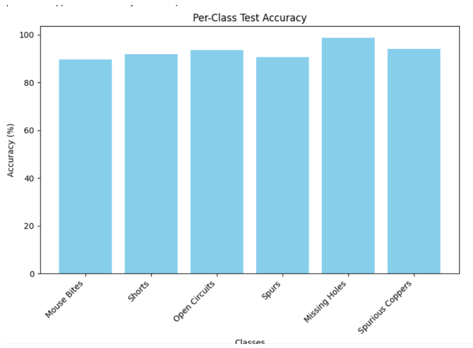

Figure 1: Per-Class Test Accuracy.

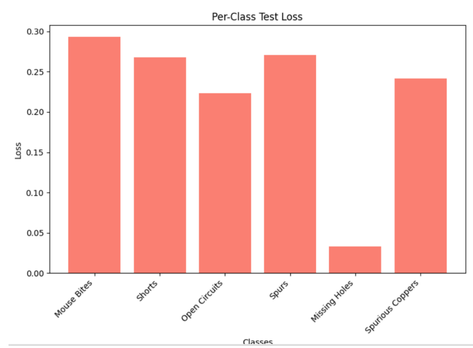

Figure 2: Per-Class Test Loss.

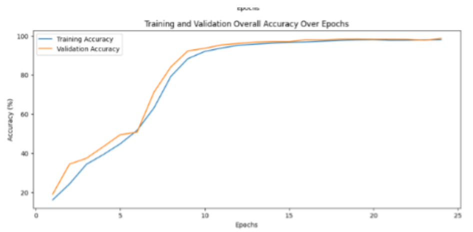

Figure 3: Training and Validation Accuracy over Epoch

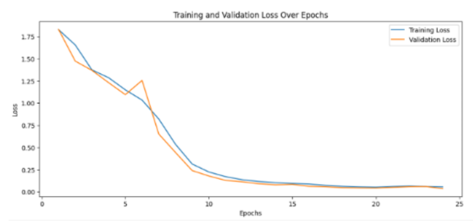

Figure 4: Training and Validation Loss over Epoch

5.3 Training and Validation Analysis

The training and validation curves (Figures 3 and 4) illustrate the learning behavior of the model across epochs:

- **Training and Validation Accuracy:** The model showed a steady increase in both training and validation accuracy, reaching convergence around epoch 20. This consistent improvement highlights the effectiveness of the model's learning capacity without significant overfitting.
- **Training and Validation Loss:** Both training and validation loss curves decreased progressively, indicating effective learning. After epoch 20, the loss values plateaued, signifying that further training beyond this point offered diminishing returns.

5.4 Discussion

The per-class performance revealed variability in the model's ability to classify certain defect types, with Missing Holes standing out as the most accurately classified defect, while Mouse Bites posed a greater challenge. The balanced trend between training and validation performance suggests that the model maintained generalization without overfitting, which was further supported by the absence of divergence between training and validation metrics over epochs.

The promising performance across various metrics positions this model as a reliable tool for defect classification. However, further improvements may focus on enhancing the precision for challenging classes such as Mouse Bites through additional data augmentation, feature extraction, or algorithmic adjustments.

6 Proposed Model Extension

1. Since the training process is highly influenced by unlabeled samples, data-expanding strategy should be helpful to further augment our dataset, thus improving model performance.
2. Inspired by ViT models, selectively masking or substituting regions of the PCB image may help the network understand context better and improve its robustness against occlusion and noise.

3. Mosaic data augmentation is widely used in models like YOLOv5 and imrpoves performance by combining different images. This is particularly useful in defect detection, where data diversity is often limited.
4. Using more advanced Loss functions should give birth to better training result. Replace the standard loss function with the Complete Intersection over Union (CIoU) loss, which has shown to be effective in models like YOLOv4 and YOLOv5 for accurately locating object boundaries.
5. Adding an FPN layer to ResNet50 can improve multi-scale detection, allowing the model to identify defects of varying sizes by merging information from multiple layers.
6. Incorporating attention modules like the Squeeze-and-Excitation (SE) or Convolutional Block Attention Module (CBAM) can help ResNet50 better focus on critical regions and enhance feature extraction. These modules have shown success in improving the accuracy of defect detection by selectively emphasizing important features.
7. Replacing parts of ResNet50 with MobileNetV2 layers can reduce model size and speed up processing. MobileNetV2's inverted residuals and linear bottlenecks help maintain accuracy while being more resource-efficient, which is advantageous for real-time applications.
8. If computational resources permit, we consider replacing ResNet50 with a hybrid backbone such as Swin Transformer, which performs well on both large and small defect detection tasks. Further experiments are required.

7 Division of work

1. Zepeng Zhao: Literature review, and proposed model extension
2. Frank Hu: Introduction, baseline model selection and description
3. Lehong Wang: Mathematical description, report formatting
4. Sungmyeon Park: Baseline model implementation

References

[1] Kang An and Yanping Zhang. Lpvit: a transformer based model for pcb image classification and defect detection. *IEEE Access*, 10:42542–42553, 2022.

[2] Wei Chen, Zhongtian Huang, Qian Mu, and Yi Sun. Pcb defect detection method based on transformer-yolo. *IEEE Access*, 10:129480–129489, 2022.

[3] Xing Chen, Yonglei Wu, Xingyou He, and Wuyi Ming. A comprehensive review of deep learning-based pcb defect detection. *IEEE Access*, 2023.

[4] R Girshick. Fast r-cnn. *arXiv preprint arXiv:1504.08083*, 2015.

[5] Ross Girshick, Jeff Donahue, Trevor Darrell, and Jitendra Malik. Rich feature hierarchies for accurate object detection and semantic segmentation. In *Proceedings of the IEEE conference on computer vision and pattern recognition*, pages 580–587, 2014.

[6] Kaiming He, Xiangyu Zhang, Shaoqing Ren, and Jian Sun. Deep residual learning for image recognition. *Proceedings of the IEEE conference on computer vision and pattern recognition*, pages 770–778, 2016.

[7] Jing Li, Weiye Li, Yingqian Chen, and Jinan Gu. Research on object detection of pcb assembly scene based on effective receptive field anchor allocation. *Computational Intelligence and Neuroscience*, 2022(1):7536711, 2022.

[8] JiaYou Lim, JunYi Lim, Vishnu Monn Baskaran, and Xin Wang. A deep context learning based pcb defect detection model with anomalous trend alarming system. *Results in Engineering*, 17:100968, 2023.

[9] Songtao Liu, Di Huang, and Yunhong Wang. Learning spatial fusion for single-shot object detection. *arXiv preprint arXiv:1911.09516*, 2019.

[10] Wei Liu, Dragomir Anguelov, Dumitru Erhan, Christian Szegedy, Scott Reed, Cheng-Yang Fu, and Alexander C Berg. Ssd: Single shot multibox detector. In *Computer Vision–ECCV 2016: 14th European Conference, Amsterdam, The Netherlands, October 11–14, 2016, Proceedings, Part I 14*, pages 21–37. Springer, 2016.

[11] Wei Liu, Dragomir Anguelov, Dumitru Erhan, Christian Szegedy, Scott Reed, Cheng-Yang Fu, and Alexander C. Berg. *SSD: Single Shot MultiBox Detector*, page 21–37. Springer International Publishing, 2016.

[12] Ze Liu, Han Hu, Yutong Lin, Zhuliang Yao, Zhenda Xie, Yixuan Wei, Jia Ning, Yue Cao, Zheng Zhang, Li Dong, et al. Swin transformer v2: Scaling up capacity and resolution. In *Proceedings of the IEEE/CVF conference on computer vision and pattern recognition*, pages 12009–12019, 2022.

[13] J Redmon. You only look once: Unified, real-time object detection. In *Proceedings of the IEEE conference on computer vision and pattern recognition*, 2016.

[14] Joseph Redmon and Ali Farhadi. Yolo9000: better, faster, stronger. In *Proceedings of the IEEE conference on computer vision and pattern recognition*, pages 7263–7271, 2017.

[15] Shaoqing Ren, Kaiming He, Ross Girshick, and Jian Sun. Faster r-cnn: Towards real-time object detection with region proposal networks. *IEEE transactions on pattern analysis and machine intelligence*, 39(6):1137–1149, 2016.

[16] Sachin Sharma, Dhruv Patel, and Dharmesh Shah. Automated detection and classification of defects in pcb using deep learning techniques: A comparison of resnet50v1 and efficientdet d1. *2023 9th IEEE India International Conference on Power Electronics (IICPE)*, pages 1–6, 2023.

[17] Amila Silva et al. Noise-robust learning from multiple unsupervised sources of inferred labels. In *Proceedings of the AAAI Conference on Artificial Intelligence*, volume 36, 2022.

[18] H. Song, M. Kim, D. Park, Y. Shin, and J.-G. Lee. Learning from noisy labels with deep neural networks: A survey. *IEEE Transactions on Neural Networks and Learning Systems*, 34(11):8135–8153, 2023.

[19] E. Strelcenia and S. Prakoonwit. A survey on gan techniques for data augmentation to address the imbalanced data issues in credit card fraud detection. *Machine Learning and Knowledge Extraction*, 5(1):304–329, 2023.

[20] Yusen Wan, Liang Gao, Xinyu Li, and Yiping Gao. Semi-supervised defect detection method with data-expanding strategy for pcb quality inspection. *Sensors*, 22(20):7971, 2022.

[21] Xiaoqi Wang, Xiangyu Zhang, and Ning Zhou. Improved yolov5 with bifpn on pcb defect detection. In *2021 2nd International Conference on Artificial Intelligence and Computer Engineering (ICAICE)*, pages 196–199. IEEE, 2021.

[22] P. Wei, C. Liu, M. Liu, Y. Gao, and H. Liu. Cnn-based reference comparison method for classifying bare pcb defects. *The Journal of Engineering*, 2018(16):1528–1533, 2018.

[23] Ligang Wu, Liang Zhang, and Qian Zhou. Printed circuit board quality detection method integrating lightweight network and dual attention mechanism. *IEEE Access*, 10:87617–87629, 2022.

[24] Haojia Xin, Zibo Chen, and Boyuan Wang. Pcb electronic component defect detection method based on improved yolov4 algorithm. In *Journal of Physics: Conference Series*, volume 1827, page 012167. IOP Publishing, 2021.

[25] Yujie Yang and Haiyan Kang. An enhanced detection method of pcb defect based on improved yolov7. *Electronics*, 12(9):2120, 2023.

[26] Yue Zhang, Fei Xie, Lei Huang, Jianjun Shi, Jiale Yang, and Zongan Li. A lightweight one-stage defect detection network for small object based on dual attention mechanism and pafpn. *Frontiers in Physics*, 9:708097, 2021.

[27] Yongbing Zhou, Minghao Yuan, Jian Zhang, Guofu Ding, and Shengfeng Qin. Review of vision-based defect detection research and its perspectives for printed circuit board. *Journal of Manufacturing Systems*, 70:557–578, 2023.